DOI: 10.1002/ejic.200900485

Maleamate(–1) and Maleate(–2) Copper(II)–2,2′-Bipyridine Complexes: Synthesis, Reactivity and Structural and Physical Studies

Katerina N. Lazarou,[a] Athanassios K. Boudalis,[a] Spyros P. Perlepes,[b] Aris Terzis,[a] and Catherine P. Raptopoulou*[a]

Keywords: Amides / Hydrolysis / Copper / Magnetic properties

A systematic investigation of the 1:2:1:2 $Cu(NO_3)\cdot 2.5H_2O$/H_2L/bpy/$LiOH\cdot H_2O$ (H_2L = maleamic acid) reaction system in $MeCN/H_2O$ was carried out. The compounds $[Cu_2(HL)_2(bpy)_2(H_2O)_2](NO_3)_2$ (**1**), $[Cu_2(HL)_2(bpy)_2(H_2O)_2](NO_3)_2\cdot 2H_2O$ (**1**·2H_2O), $[Cu_2Li_2(L')_2(bpy)_2(H_2O)_6][Cu_2(HL)_2(bpy)_2(H_2O)_2](NO_3)_4$ (**2**), $[Cu_4(L')_2(NO_3)_2(bpy)_4(H_2O)_2](NO_3)_2\cdot 2H_2O$ (**3**·2H_2O) and $[Cu(L')(bpy)]_n\cdot 2nH_2O$ (**4**·2nH_2O) were isolated, depending on the crystallization method employed. Complexes **2**, **3**·2H_2O and **4**·2nH_2O contain the maleate(–2) anion (L'^{2-}), which was formed in situ through metal-ion-assisted hydrolysis of the primary amide group of H_2L. Efforts to prepare complex **3** from the direct use of maleic acid (H_2L') afforded compounds **4**·2nH_2O, $[Cu_4(L')_2(NO_3)_2(bpy)_4(H_2O)_2](NO_3)_2\cdot 2[Li(NO_3)(H_2O)_3]\cdot 4H_2O$ (**5**·4H_2O) and $[Cu(NO_3)(bpy)(H_2O)_3](NO_3)$ (**6**) from the 1:1:1:2 $Cu(NO_3)\cdot 2.5H_2O/H_2L'$/bpy/$LiOH\cdot H_2O$ reaction system in $MeCN/H_2O$. The maleamate(–1) ligand presents the less common $\eta^1{:}\mu_2$ coordination mode in the cations of **1**, **1**·2H_2O and **2**. The maleate(–2) ligand exhibits the $\eta^1{:}\eta^1{:}\eta^1{:}\eta^1{:}\mu_3$ coordination mode in the $[Cu^{II}_4]$ cations of **3**·2H_2O and **5**·4H_2O and in the $[Cu^{II}_2Li^{I}_2]$ heterometallic cation of **2**. The crystal structures of the complexes are stabilized by various H-bonding patterns. Characteristic IR bands of the complexes are discussed in terms of the known structures and the coordination modes of the ligands. Magnetic susceptibility measurements for **3**·2H_2O reveal weak ferromagnetic interactions along the periphery of the Cu_4 rhombus (J = 3.3 cm^{-1}, $-2J_{ij}S_iS_j$ Hamiltonian formalism), which stabilizes an S = 2 ground state.

Introduction

Metal carboxylates represent a fruitful source for molecular clusters[1] and coordination polymers,[2] whose aesthetic beauty and structural complexity is closely related to their physical properties. Outstanding in the field are the α,ω-dicarboxylate ligands, because (i) the presence of the two carboxylato moieties, (ii) the relative orientation of the two carboxylato groups, (iii) the mono- or dianionic forms, (iv) the possibility of various coordination modes, and (v) their ability to form secondary building blocks enhance the construction of novel multidimensional architectures.[3] The conformational flexibility (for $n \geq 1$ in **I**, Scheme 1) or the π-induced rigidity of the carbon skeleton (e.g. **II**–**IV**, Scheme 1) offer additional variables that can influence the structural characteristics of the metal complexes. Moreover, the combination of the α,ω-dicarboxylates, such as **I**–**IV** in Scheme 1, with aromatic bidentate *N*,*N*′-chelates (e.g. 2,2′-bipyride, 1,10-phenanthroline) has led to a variety of structures.[4]

On the other hand, *the coordination chemistry of the monoamides of the aliphatic α,ω-dicarboxylates has been scarcely investigated* [e.g. $^-OOC–(CH_2)_n–CONH_2$ **V**, n = 2,3,4,5,...; $^-OOC–CH{=}CH–CONH_2$ **VI**, fumarate monoamide; **VII** maleate monoamide or maleamate; $^-OOC–C{\equiv}C–CONH_2$ **VIII**, acetylene dicarboxylate monoamide; Scheme 1]. These types of ligands are expected to yield metal complexes with different chemical and structural features than those of the α,ω-dicarboxylates, because of the different charge, electronic properties and hydrogen bonding ability of the amide group.

Keeping these in mind, we have embarked in a research programme aiming at the investigation of the coordination chemistry of the monoamides of aliphatic α,ω-dicarboxylates in the presence of aromatic bidentate *N*,*N*′- or tridentate *N*,*N*′,*N*′′-chelates. Our efforts have yielded metal complexes that exhibit a variety of structural features, as far as nuclearity and dimensionality are concerned, because of the coordination versatility of the carboxylato group and the hydrogen bonding ability of the amide group. We have explored ligand systems involving the succinamate(–1) (n = 2 in **V** of Scheme 1, $Hsucm^-$)[5] and the maleamate(–1) (**VII** in Scheme 1, HL^-) ligands[6] in combination with aromatic bidentate *N*,*N*′- or tridentate *N*,*N*′,*N*′′-chelates. We have examined the influence of various synthetic parameters, such as the reaction solvent, the presence or absence of external

[a] Institute of Materials Science, NCSR "Demokritos", 15310 Aghia Paraskevi, Athens, Greece
Fax: +30-210-6519430
E-mail: craptop@ims.demokritos.gr
[b] Department of Chemistry, University of Patras, 26504 Patras, Greece
Supporting information for this article is available on the WWW under http://dx.doi.org/10.1002/ejic.200900485.

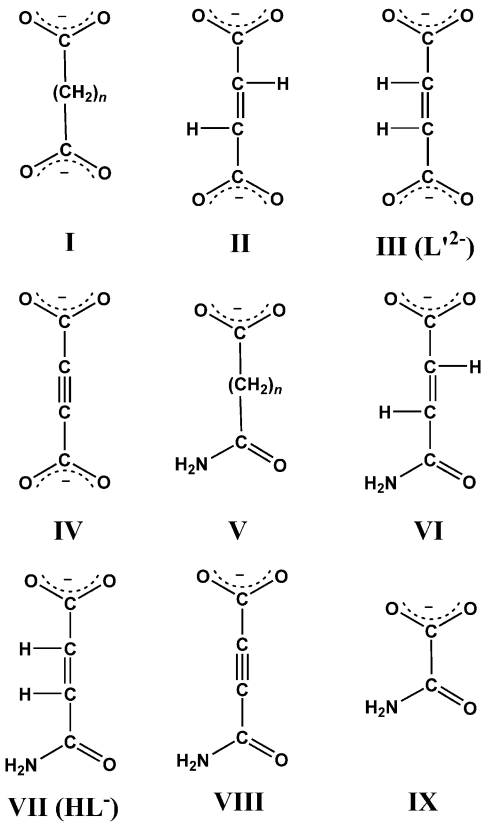

Scheme 1. Some of the ligands discussed in the text. The ligands used in this work are the maleate(–2) (**III**, L'^{2-}) and maleamate(–1) (**VII**, HL^-) ions.

hydroxides, the inorganic anion in the metal salt, the stoichiometry of the reactants, the nature of the aromatic N-donor ligands and the crystallization method, on the identity of the products.

We present herein our results from the study of the $Cu(NO_3)_2{\cdot}2.5H_2O/H_2L/bpy/LiOH{\cdot}H_2O$ reaction system, which has afforded interesting compounds that contain intact HL^- and/or the maleate(–2) ligand (**III**, L'^{2-}; Scheme 1) i.e. compounds $[Cu_2(HL)_2(bpy)_2(H_2O)_2](NO_3)_2$ (**1**), $[Cu_2(HL)_2(bpy)_2(H_2O)_2](NO_3)_2{\cdot}2H_2O$ (**1**·2H_2O), $[Cu_2Li_2(L')_2(bpy)_2(H_2O)_6][Cu_2(HL)_2(bpy)_2(H_2O)_2](NO_3)_4$ (**2**), and $[Cu_4(L')_2(NO_3)_2(bpy)_4(H_2O)_2](NO_3)_2{\cdot}2H_2O$ (**3**·2H_2O); L'^{2-} was formed in situ through metal-ion-assisted hydrolysis of the primary amide group. Our efforts to prepare pure **3** from the direct use of H_2L', for further physical studies, afforded complex $[Cu_4(L')_2(NO_3)_2(bpy)_4(H_2O)_2](NO_3)_2{\cdot}2[Li(NO_3)(H_2O)_3]{\cdot}4H_2O$ (**5**·4H_2O). We illustrate the syntheses of the above complexes, their structural and spectroscopic characterization, and the magnetic study of **3**, and we discuss our results with respect to our previous work.

Results and Discussion

Syntheses of the Complexes

Our previous investigation of the tertiary $CuX_2{\cdot}xH_2O/H_2L/phen$ (X^- = Cl^-, NO_3^-, ClO_4^-) and $Cu(ClO_4)_2{\cdot}6H_2O/H_2L/bpy$ reaction systems[6b,6c] led to interesting results concerning the chemical and structural properties of the compounds isolated. In order to examine the extent to which the nature of the inorganic anion of copper(II) might affect the identity of the products from the bpy-containing reaction system, we have expanded our research to the use of $Cu(NO_3)_2{\cdot}2.5H_2O$.

Our initial efforts involved the reaction of $Cu(NO_3)_2{\cdot}2.5H_2O$ with 2 equiv. H_2L and 1 equiv. bpy in the presence of 2 equiv. $LiOH{\cdot}H_2O$ in $MeCN/H_2O$ (10:1 v/v). We isolated *five* different products from the same reaction mixture, depending on the crystallization method employed: (i) layering of the resultant blue solution with a mixture of Et_2O/*n*-hexane afforded blue prismatic crystals of $[Cu_2(HL)_2(bpy)_2(H_2O)_2](NO_3)_2{\cdot}2H_2O$ (**1**·2H_2O), (ii) vapour diffusion of the reaction solution with Et_2O gave a mixture of blue prismatic crystals of **1**·2H_2O and dark blue needlelike crystals of $[Cu_2Li_2(L')_2(bpy)_2(H_2O)_6][Cu_2(HL)_2(bpy)_2(H_2O)_2](NO_3)_4$ (**2**) in an approximate 1:1 ratio, (iii) slow evaporation of the reaction solution at room temperature afforded blue crystals of $[Cu_2(HL)_2(bpy)_2(H_2O)_2](NO_3)_2$ (**1**), (iv) storage at ca. 4 °C gave $[Cu_4(L')_2(NO_3)_2(bpy)_4(H_2O)_2](NO_3)_2{\cdot}2H_2O$ (**3**·2H_2O), and (v) storage of the reaction solution in closed vials at room temperature afforded the known complex[7] $[Cu(L')(bpy)]_n{\cdot}2nH_2O$ (**4**·2*n*H_2O) (Scheme 2).

Compounds **1** and **1**·2H_2O contain the same dinuclear cation; the presence of two water solvate molecules in the structure of the latter leads to a completely different crystal structure as a result of hydrogen-bonding interactions.

Complex **2** is quite impressive because it consists of two cationic complexes, one of which contains the maleamate(–1) ligand (HL^-, **VII** in Scheme 1) and is analogous to the cation of **1**·2H_2O and a second that contains the maleate(–2) ligand (L'^{2-}, **III** in Scheme 1); the latter ligand is also present in complex **3**. The dianion of L'^{2-} in **2** and **3** was formed in situ by the hydrolysis of the primary amide group of H_2L to the carboxylate function. It is well known that such hydrolysis reactions are accelerated by metal ions.[8] We believe that the little amount of water added in the reaction mixture – in order to dissolve $LiOH{\cdot}H_2O$ and to prevent contamination of the product by $LiNO_3$, which is insoluble in anhydrous MeCN – or contained in the starting materials is beneficial to the hydrolysis of the primary amide group and the to the formation of the maleate(–2) ligand followed by its subsequent coordination, which affords **2** and **3**·2H_2O. The Cu^{II}-assisted/promoted $HL^- \rightarrow L'^{2-}$ transformation was also observed in the case of the $Cu(ClO_4)_2{\cdot}6H_2O/H_2L/bpy/OH^-$ reaction system.[6c]

In all cases above, the reaction mixture was gently heated before the crystallization process. By avoiding heating, pure **1**·2H_2O was obtained from the 1:2:1:2 $Cu(NO_3)_2{\cdot}2.5H_2O/H_2L/bpy/LiOH{\cdot}H_2O$ reaction mixture, i.e. the compounds **2**, **3**·2H_2O and **4**·2*n*H_2O, which contain the maleate(–2) ligand, were not isolated. Without any mechanistic implications, we assume that the gentle heating of the reaction mixture, along with the simultaneous presence of Cu^{II} ions, may have facilitated the $HL^- \rightarrow L'^{2-}$ transformation.

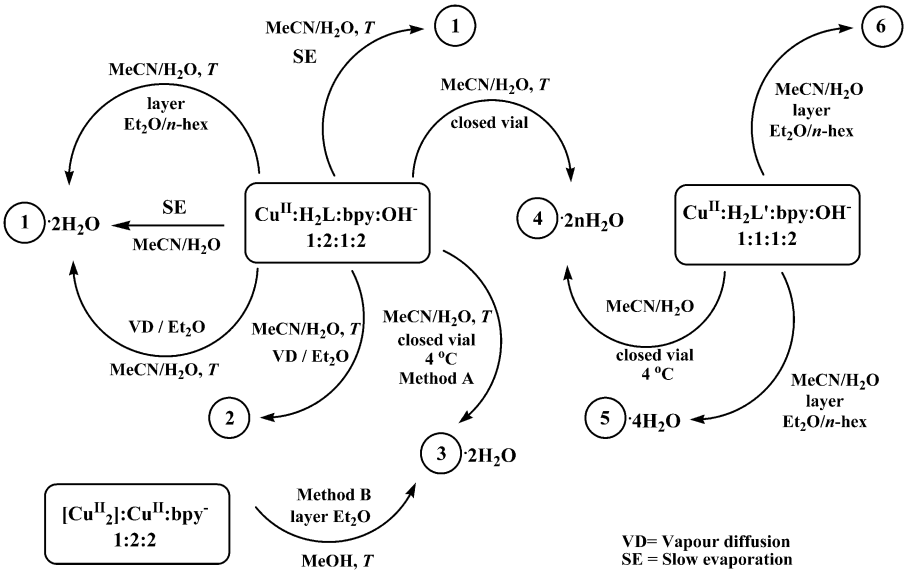

Scheme 2. Diagram of the reaction pathways discussed in the text.

In order to prepare pure **3**·2H_2O in a rational manner, we used the known complex[6c] [$Cu_2(L')_2(bpy)_2$]·2MeOH {which includes the maleate(–2) dianion} as starting material; its reaction with 2 equiv. $Cu(NO_3)_2$·2.5H_2O and 2 equiv. bpy in MeOH affords pure **3**·2H_2O.

In a next step, we wondered whether the direct use of H_2L' might lead to the isolation of **3**, and we employed the reaction of $Cu(NO_3)_2$·2.5H_2O with 1 equiv. H_2L' and 1 equiv. bpy in the presence of 2 equiv. LiOH·H_2O in MeCN/H_2O. *Three* different compounds were isolated from the same light blue reaction solution, depending on the crystallization method employed: (i) layering of the reaction solution with a mixture of Et_2O/*n*-hexane afforded a mixture of blue crystals of [$Cu_4(L')_2(NO_3)_2(bpy)_4(H_2O)_2$]-($NO_3$)$_2$·2[$Li(NO_3)(H_2O)_3$]·4$H_2O$ (**5**·4H_2O) and light blue-greenish platelike crystals of the known[9] complex [$Cu(NO_3)(bpy)(H_2O)_3$](NO_3) (**6**) in an approximate 1:1 ratio, and (ii) storage of the reaction solution in closed vials at ca. 4 °C gave the known compound[7] [$CuL'(bpy)]_n$·2*n*H_2O (**4**·2*n*H_2O). Complex **5** is quite impressive because it contains a tetranuclear cation, analogous to that of **3** and neutral Li^I complex molecules.

The isolation of *five* different compounds, i.e. **1**, **1**·2H_2O, **2**, **3**·2H_2O and **4**·2*n*H_2O, from the $Cu(NO_3)_2$·2.5H_2O/H_2L/bpy/LiOH·H_2O reaction mixture in MeCN/H_2O, under different crystallization conditions, constitutes an excellent example of rich coordination chemistry. In addition, the isolation of *three* different compounds comprising various species, i.e. a Cu^{II}_4 cation and two neutral Li^I complex molecules in **5**, a 1D complex (**4**·2*n*H_2O) and a mononuclear maleate-free complex (**6**) from the $Cu(NO_3)_2$·2.5H_2O/H_2L'/bpy/LiOH·H_2O reaction mixture in MeCN/H_2O by different crystallization conditions is also remarkable. It is well known that solutions of transition-metal ions and one or more ligands can give complicated mixtures of products in equilibrium – as a result of the labile nature of the metal–ligand bonds and other noncovalent bonds that may eventually form (H bonds, π–π stacking etc); the case is further complicated when metal-ion-assisted ligand transformations and/or other reactivity processes also take place. From this multitude of products, it is often possible to isolate one or more compounds by their selective precipitation and subsequent crystallization, although it still remains a challenge to isolate different species from the same reaction mixture, and more so to structurally characterize them.[10] We came across an analogous behaviour during the investigation of the $CuCl_2$/H_2mal/phen/LiOH·H_2O reaction system in MeOH (H_2mal = malonic acid) from which seven different products were isolated on the basis of their different solubility.[11] The present reaction system involving H_2L is much more complicated and interesting, since the observed Cu^{II}-assisted $HL^- \rightarrow L'^{2-}$ transformation simultaneously yields ligands with different coordination and electronic properties; the coordination properties of the ligands is reflected by the isolation of species common in both reaction systems examined; thus complex **4**·2*n*H_2O was isolated from both HL^-- and L'^{2-}-containing reaction systems, while the Cu^{II}_4 cation present in **3** and **5** was obtained from HL^-- and L'^{2-}-containing reaction systems, respectively. Both reaction systems represent excellent examples of dynamic mixtures of various species in equilibrium, from which we were able to isolate a multitude of products on the basis of their selective crystallization.

Description of the Structures

The molecular structures of the dinuclear cations that are present in complexes **1** and **1**·2H_2O are very similar. We give below a comparative structural description for the cations of **1** (Figure 1) and **1**·2H_2O (Figure S1). The structure of the cation in both complexes consists of two centrosym-

metrically related Cu^{II} ions bridged by the carboxylate groups of two HL^- ligands that present the less common η^1:μ_2 coordination mode [Cu1···Cu1′ = 3.346(3) and 3.369(5) Å in **1** and **1**·2H_2O, respectively]. A chelating bpy and a water molecule complete the five-coordination around each Cu^{II} atom. The neutral primary amide groups of the HL^- ligands remain uncoordinated. The Cu···O2 distance of 2.861(3) Å in **1** (dashed line in Figure 1) provides evidence for a weak interaction, as has sometimes[12] (but not always[13]) been observed for monatomic bridging carboxylate groups. The coordination geometry about each metal ion in both complexes is well described as square pyramidal, in which the bridging carboxylate oxygen atoms occupy the apical positions for the two Cu^{II} centres; for example, in **1**, atoms O1 and O1′ occupy the apical positions for Cu1 and Cu1′, respectively. Analysis of the shape-determining angles by using the approach of Reedijk, Addison and co-workers[14] yields values for the trigonality index, τ, of 0.17 and 0.21 for the Cu^{II} ions in **1** and **1**·2H_2O, respectively. The Cu–N and Cu–O bond lengths are in the range 1.960(2)–2.310(2) Å in **1** and 1.966(3)–2.351(3) Å in **1**·2H_2O (Table S1). As expected, the axial bonds are the longest. The structures of the cations of **1** and **1**·2H_2O are quite similar to the structures of the cations in $[Cu_2(LH)_2(bpy)_2(H_2O)_2](ClO_4)_2$ and $[Cu_2(LH)_2(bpy)_2(H_2O)_2](ClO_4)_2 \cdot 2H_2O$, previously reported by us.[6c]

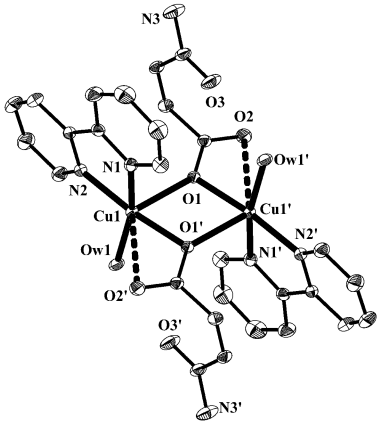

Figure 1. Partially labelled plot of the cation of **1** with ellipsoids drawn at the 30% probability level. H atoms have been omitted for clarity. Primed atoms are generated by the symmetry operation 1 – *x*, 1 – *y*, –*z*.

In the crystal lattice of **1**, intermolecular hydrogen-bonding interactions are observed, which form a 2D network parallel to the (100) plane (Figure 2, Table S5). In the crystal lattice of **1**·2H_2O, intra- [O3···Ow1] and intermolecular hydrogen-bonding interactions [N3···O3 (–*x*, –*y*, *z*)] form 1D chains parallel to the *b* axis, which are further associated and form a 2D network extending parallel to the (001) plane (Figure 3, Table S5).

The structure of complex **2** consists of heterometallic tetranuclear cations $[Cu_2Li_2(L')_2(bpy)_2(H_2O)_6]^{2+}$ (Figure 4), dinuclear cations $[Cu_2(HL)_2(bpy)_2(H_2O)_2]^{2+}$ similar to

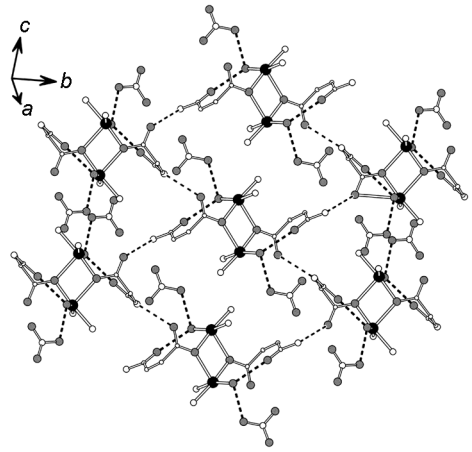

Figure 2. A part of the 2D structure of **1** showing the H-bonding interactions. Colour code: Cu, black; O, medium grey; N, large white; C, small white. H bonds are presented by dashed lines. Only the N atoms of the bpy ligands are shown.

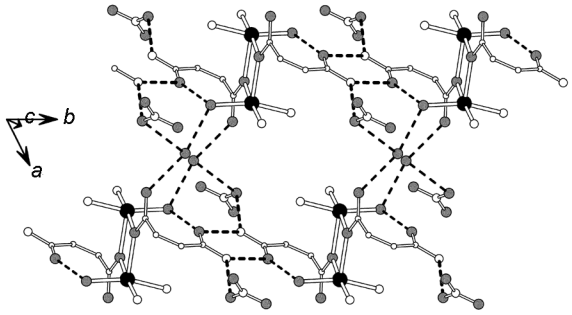

Figure 3. A part of the 2D structure of **1**·2H_2O showing the H-bonding interactions. Colour code: Cu, black; O, medium grey; N, large white; C, small white. H bonds are presented by dashed lines. Only the N atoms of the bpy ligands are shown.

those present in complexes **1** and **1**·2H_2O (Figure 1), and nitrate counterions; the latter two will not be discussed further.

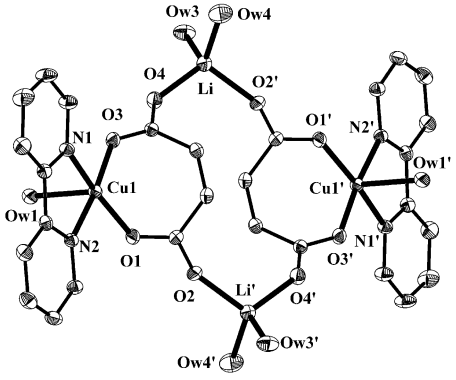

Figure 4. Partially labelled plot of the $Cu^{II}_2Li^{I}_2$ cation of **2** with ellipsoids drawn at the 30% probability level. H atoms have been omitted for clarity. Primed atoms are generated by the symmetry operation –*x*, –*y*, 1 – *z*.

The molecular structure of the heterometallic cation consists of a centrosymmetric cyclic $Cu^{II}_2Li^{I}_2$ unit; the metal ions are held together through two $\eta^1:\eta^1:\eta^1:\eta^1:\mu_3$ L'^{2-} ligands. The coordination geometry around each Cu^{II} ion is square pyramidal (τ = 0.14). The basal positions of the square pyramid are occupied by the nitrogen atoms of a bpy molecule and atoms O1 and O3 of the L'^{2-} ligand, while the apical position is occupied by a coordinated H_2O molecule. The Cu–N and Cu–O bond lengths are in the range 1.916(3)–2.275(4) Å (Table S2). The coordination geometry around each Li^{I} ion is tetrahedral and comprises the oxygen atoms O4 and O2′ belonging to two L'^{2-} ligands and two coordinated H_2O molecules [Li–O 1.914(8)–1.967(9) Å]. The structure of the heterometallic tetranuclear cation $[Cu_2Li_2(L')_2(bpy)_2(H_2O)_6]^{2+}$ is similar to the structure of the neutral complex $[Cu_2Li_2Cl_2(mal)_2(phen)_2(MeOH)_4]$[11] {$mal^{2-}$ = malonate(–2) ligand}.

In the lattice structure of **2**, the $Cu^{II}_2Li^{I}_2$ cations are hydrogen bonded and form 1D chains, which are further hydrogen bonded to the Cu^{II}_2 cations and the nitrate anions to form a 2D network extending parallel to the (1-10) plane (Figure 5, Table S5).

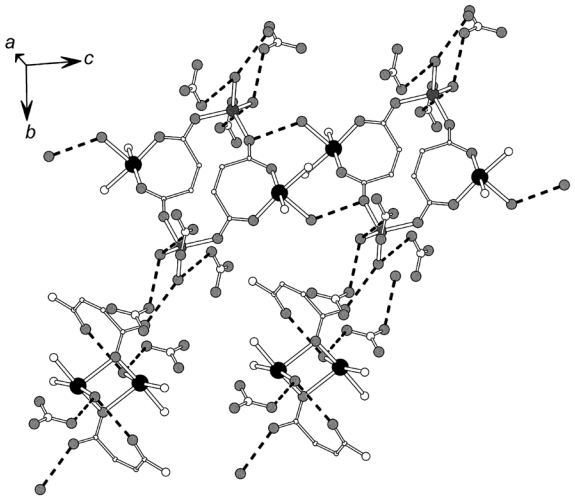

Figure 5. A part of the 2D structure of **2** showing the H-bonding interactions. Colour code: Cu, black; O, medium grey; N, large white; C, small white; Li, dark grey. H bonds are presented by dashed lines. Only the N atoms of the bpy ligands are shown.

The structure of complex **3**·2H_2O consists of tetranuclear cations $[Cu_4(L')_2(NO_3)_2(bpy)_4(H_2O)_2]^{2+}$, NO_3^- counterions and solvate H_2O molecules; the latter two will not be further discussed. Each L'^{2-} ligand adopts the $\eta^1:\eta^1:\eta^1:\eta^1:\mu_3$ coordination mode, thus bridging three Cu^{II} ions of the tetranuclear cation through the formation of a remarkable seven-membered $Cu–O_{carboxylate}–C–C=C–C–O_{carboxylate}$ chelating ring (Figure 6). A chelating bpy, an aqua ligand for both Cu1 and Cu3, and a monodentate nitrate anion for both Cu2 and Cu4, respectively, complete the pentacoordination around each metal ion, thus defining a square pyramidal geometry in which the aqua and the nitrate ligands occupy the apical position for Cu1/Cu3 and Cu2/Cu4, respectively. The Cu–N and Cu–O bond lengths are in the range 1.938(3)–2.308(4) Å (Table S3).

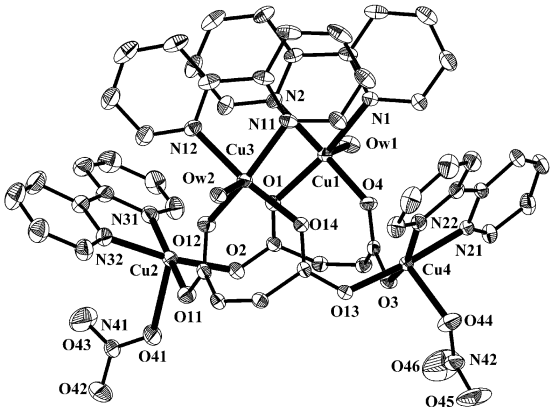

Figure 6. Partially labelled plot of the cation of **3**·2H_2O with ellipsoids drawn at the 30% probability level. H atoms have been omitted for clarity.

In the crystal lattice of **3**·2H_2O, the presence of intermolecular hydrogen-bonding interactions between the tetranuclear cations, the nitrates and the solvate H_2O molecules result in the formation of a 3D network (Figure 7, Table S5).

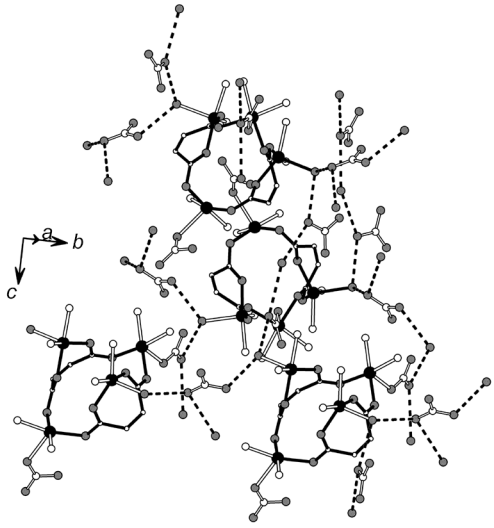

Figure 7. A part of the 3D structure of **3**·2H_2O showing the H-bonding interactions. Colour code: Cu, black; O, medium grey; N, large white; C, small white. H bonds are presented by dashed lines. Only the N atoms of the bpy ligands are shown.

The structure of complex **5**·4H_2O consists of centrosymmetric tetranuclear cations $[Cu_4(L')_2(NO_3)_2(bpy)_4(H_2O)_2]^{2+}$ analogous to those present in complex **3**·2H_2O, two neutral $[Li(NO_3)(H_2O)_3]$ complexes (Figure 8), NO_3^- counterions and H_2O solvate molecules. The Cu–N and Cu–O bond lengths in the $[Cu_4]$ cation are in the range 1.954(3)–2.278(4) Å (Table S4). The coordination geometry around the Li^{I} ion is tetrahedral and comprises three aqua ligands and a monodentate nitrate group [Li–O 1.921(10)–2.007(10) Å].

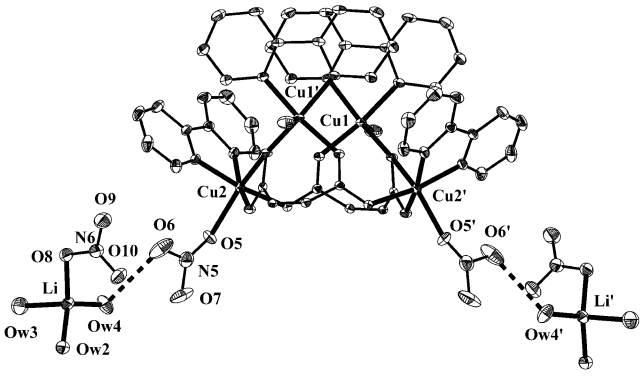

Figure 8. Partially labelled plot of the Cu^{II}_4 cation and the Li^I complex molecule of **5**·4H_2O with ellipsoids drawn at the 30% probability level. H atoms have been omitted for clarity. Primed atoms are generated by the symmetry operation $-x$, y, $0.5 - z$. H bonds between the Cu^{II}_4 and Li^I units are shown as dashed lines.

In the crystal lattice of **5**·4H_2O, an extensive network of hydrogen-bonding interactions involving the Cu^{II}_4 and Li^I complexes, as well as the NO_3^- counterions and the solvate H_2O molecules, result in the formation of a 3D network (Figure 9, Table S5).

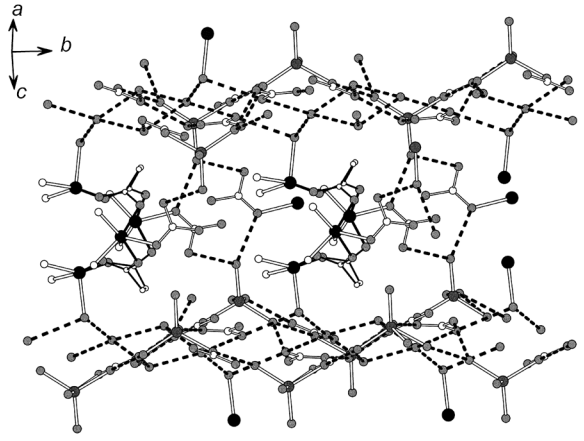

Figure 9. A part of the 3D structure of **5**·4H_2O showing the H-bonding interactions. Colour code: Cu, black; O, medium grey; N, large white; C, small white; Li, dark grey. H bonds are presented by dashed lines. Only the N atoms of the bpy ligands are shown.

IR Spectroscopy

Dried samples of complexes **1**, **1**·2H_2O, **2**, **3**·2H_2O and **5**·4H_2O were characterized by IR spectroscopy. All complexes exhibit a very broad band covering the range 3450–3150 cm^{-1}, which can be assigned to ν(OH) vibrations of lattice and/or coordinated H_2O.[15] The broadness and relatively low frequency of this band are both indicative of H bonding.

All spectra exhibit the characteristic ν(C=C) and ν(C=N) bands of bpy in the 1600–1400 cm^{-1} region, which are sensitive to chelation.[16] The strong band at ca. 1380 cm^{-1} in all spectra is attributed[17] to the $\nu_3(E')$[ν_d(NO)] mode of the uncoordinated D_{3h} ionic nitrates. In the spectra of **3**·2H_2O and **5**·4H_2O, the bands at ca. 1445 and 1315 cm^{-1} are assigned[17] to the $\nu_2(B_2)$ [$\nu_{as}(NO_2)$] and $\nu_1(A_1)$ [$\nu_s(NO_2)$] bands, respectively; the small difference (ca. 130 cm^{-1}) in the position of the bands is consistent with the presence of monodentate coordinated NO_3^- groups of C_{2v} symmetry in these compounds.[17] Complexes **3**·2H_2O and **5**·4H_2O have uncoordinated ionic nitrates as counterions as well as coordinated NO_3^- groups. As a result, in the spectra of these compounds, there are bands that can be attributed to both groups.

The typical bands of the neutral amide group, i.e. $\nu_{as}(NH_2)$, $\nu_s(NH_2)$, ν(C=O) and ν(CN), in the spectra of **1**, **1**·2H_2O and **2** (Table S6) are located at almost the same wavenumber as those in the spectrum of Na(HL), which confirms the crystallographically established nonparticipation of the amide group in coordination. The difference Δ, where $\Delta = \nu_{as}(CO_2) - \nu_s(CO_2)$, for **1** (221 cm^{-1}), **1**·2H_2O (219 cm^{-1}) and **2** (220 cm^{-1}) is more than that of Na(HL), as expected for the crystallographically confirmed, essentially monatomic bridging mode of the carboxylate ligation.[5,18]

The difference Δ for **3**·2H_2O (116 cm^{-1}) and **5**·4H_2O (112 cm^{-1}) is much smaller than that of the "free" maleate-(–2) ion (200 cm^{-1})[7a] (Table S7), as expected for the bidentate bridging mode of the carboxylate ligation.[18] Owing to the presence of two different ligands (L'^{2-}, HL^-) in **2**, two $\nu_{as}(CO_2)$ and two $\nu_s(CO_2)$ bands appear in its spectrum. The pair at 1589/1414 cm^{-1} (Δ = 175 cm^{-1} <200 cm^{-1}) are assigned to the bidentate bridging carboxylate groups of the L'^{2-} ligand, while the pair at 1603/1383 cm^{-1} (Δ = 220 cm^{-1}) to the monatomic bridging carboxylate groups of HL^-.[18]

Magnetic Studies

The $\chi_M T$ product for **3**·2H_2O (0.5 T) is 1.65 $cm^3 mol^{-1} K$, in agreement with the value predicted for four noninteracting S = 1/2 ions (g = 2.1). Upon cooling, this value increases continuously up to a value of 3.03 $cm^3 mol^{-1} K$ at 2 K (Figure 10), which is in agreement with an S = 2 ground state. The overall behaviour indicates ferromagnetic interactions, albeit weak.

The symmetry of **3**·2H_2O, as revealed by its molecular structure (Figure 6), allows us to consider one coupling parameter for all exchange interactions between adjacent Cu^{II} ions along the periphery of the rhombus. Diagonal interactions were neglected because of the large Cu···Cu distances [Cu2···Cu4 7.27 Å] and/or because of the fact that possible exchange would have to be through-space and transmitted through nonmagnetic orbitals [in the case of Cu1 and Cu3]. Thus, the spin Hamiltonian used was as shown.

$\hat{H} = -2J(\hat{S}_1\hat{S}_2 + \hat{S}_2\hat{S}_3 + \hat{S}_3\hat{S}_4 + \hat{S}_4\hat{S}_1)$

Fits performed on the basis of this model yield excellent results. Best-fit parameters are J = +3.3 cm^{-1}, g = 2.123 and $R = 7.8 \times 10^{-5}$. Simulations of M vs. H data at 2 K (Figure 10, inset) based on the best-fit solution (by considering g = 2.197) or a Brillouin curve (S = 2, g = 2.197) were practically superimposable. However, at 5 K, where excited

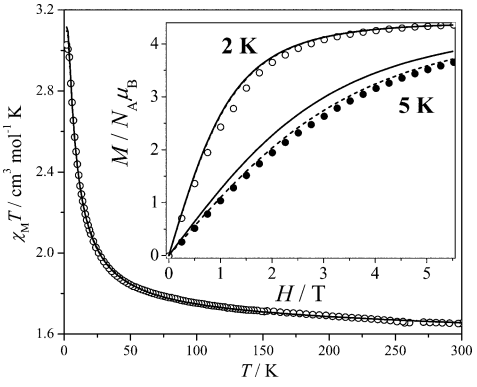

Figure 10. $\chi_M T$ vs. T data for **3**·2H_2O and the best-fit curve according to the model discussed in the text. The inset shows magnetization isotherms collected at 2 (○) and 5 (●) K. Dashed lines correspond to curves calculated according to the best-fit solution (g = 2.197). Solid lines are the Brillouin curves (S = 2, g = 2.197). At 2 K, the theoretical curves are practically superimposable; at 5 K, the Brillouin curves severely overestimate the magnetization M.

S = 1, 0 states are populated, the Brillouin curve overestimates the magnetization M.

The ferromagnetic coupling in **3**·2H_2O can be rationalized by considering the exchange pathways between the square-pyramidal Cu^{II} ions. Magnetic exchange will be transmitted through the three atoms of the *syn*,*anti* bridging carboxylates (O···C···O), which should result in a weak coupling. However, as the basal planes of the Cu^{II} coordination spheres are close to orthogonal [e.g. for Cu2 and Cu3, the dihedral angle between planes N31/N32/O11/O2 and N11/N12/O12/O14 is 84.8°], the antiferromagnetic component is expected to be negligible.

Concluding Comments and Perspectives

The use of the HL^-/bpy "ligand blend" in reactions with $Cu(NO_3)_2$·2.5H_2O yielded dinuclear, tetranuclear and polymeric complexes, i.e. the new complexes **1**, **1**·2H_2O, **2** and **3**·2H_2O and the known[7] complex **4**·2*n*H_2O. The chemistry of the $Cu(NO_3)_2$·2.5H_2O/HL^-/bpy system shows similarities and differences to that of the corresponding $Cu(ClO_4)_2$·6H_2O/HL^-/bpy system.[6c] Complexes containing the cation $[Cu_2(HL)_2(bpy)_2(H_2O)_2]^{2+}$ (**1** and **1**·2H_2O) have been isolated from both reaction systems, as well as the 1D coordination polymer $[Cu(L')(bpy)]_n$·2*n*H_2O (**4**·2*n*H_2O); L'^{2-} is the maleate(–2) ligand that was formed in situ through the Cu^{II}-assisted $HL^- \rightarrow L'^{2-}$ transformation. The replacement of ClO_4^- with the coordinatively active NO_3^- additionally afforded complex **2**, which contains both HL^- and L'^{2-} ligands, and the tetranuclear complex **3**·2H_2O, which contains exclusively L'^{2-}. All five compounds have been isolated from the same reaction solution, either as mixtures or in the pure form, depending on the crystallization method employed. Thus, the reaction system under investigation constitutes a dynamic mixture of species, whose crystallization and subsequent isolation is based on their different solubilities.

The use of the L'^{2-}/bpy "ligand blend" in reactions with $Cu(NO_3)_2$·2.5H_2O – in order to prepare **3**·2H_2O in a rational manner – yielded the new complex **5**·4H_2O and the known complexes **4**·2*n*H_2O[7]and **6**.[9] As in the HL^- reaction system, the three complexes have been isolated from the same reaction solution, either as mixtures or in the pure form, depending on their different solubilities. Complex **5**·4H_2O contains a tetranuclear cation that is structurally similar to that present in **3**·2H_2O and neutral tetrahedral Li^I complexes. The chemistry of the $Cu(NO_3)_2$·2.5H_2O/L'^{2-}/bpy system shows similarities and differences to that of the corresponding $Cu(ClO_4)_2$·6H_2O/L'^{2-}/bpy system.[6c] The common feature is the isolation of the 1D complex **4**·2*n*H_2O. The ClO_4^--containing system afforded the 1D complex $[Cu_2(L')(bpy)_2(H_2O)_2]_n(ClO_4)_{2n}$ and the dinuclear complex $[Cu_2(L')_2(bpy)_2]$, while the replacement of ClO_4^- with NO_3^- yielded the tetranuclear complex **5**·4H_2O, in which the coordination of the nitrates blocks further polymerization. The L'^{2-} ligand in the structures of **2**, **3**/**5** and **4** adopts three different coordination modes, a fact that is indicative of its coordination versatility and capability of affording various structural architectures.

The rich coordination chemistry of HL^- and the metal-ion assisted hydrolysis and methanolysis[6] of the primary amide group to the carboxylate function and the monomethyl ester, respectively [leading to the in situ formation of maleamate(–2) and monomethyl maleate(–1) ligands, respectively], that have been observed during the investigation of the CuX_2·*n*H_2O (X^- = Cl^-, ClO_4^-, NO_3^-)/H_2L/*N*,*N*′-chelate reaction systems has prompted us to investigate analogous reaction mixtures with mono- and tridentate chelating ligands; our results will be reported soon.

Experimental Section

General Procedures and Materials: All manipulations were performed under aerobic conditions by using materials as received (Aldrich Co). All chemicals and solvents were of reagent grade. Elemental analyses for C, H and N were performed on a Perkin–Elmer 2400/*II* automatic analyzer. IR spectra were recorded from KBr pellets in the range 4000–400 cm^{-1} on a Bruker Equinox 55/S FTIR spectrophotometer. $[Cu_2(L')_2(bpy)_2]$·2MeOH was prepared as previously reported.[6c] Variable-temperature magnetic susceptibility measurements were carried out on a polycrystalline sample of **3**·2H_2O in the temperature range 2.0–300 K by using a Quantum Design MPMS SQUID magnetometer under magnetic fields of 0.5, 1.0 and 1.5 T. Diamagnetic corrections for the complexes were estimated from Pascal's constants. The magnetic susceptibility was computed by exact calculation of the energy levels associated with the spin Hamiltonian, through diagonalization of the full-matrix with a general-symmetry program.[19] Least-squares fittings were accomplished with an adapted version of the function-minimization program MINUIT.[20] The error factor R is defined as $R = \Sigma\frac{(x_{exp} - x_{cal})^2}{N(x_{exp})^2}$, where N is the number of experimental points. Simulations of the magnetization M vs. applied field H were carried out with the MAGPACK program package, with parameters derived from fits of the magnetic susceptibility.[21]

Preparation of $[Cu_2(HL)_2(bpy)_2(H_2O)_2](NO_3)_2·2H_2O$ (1·2H$_2$O), and $[Cu_2Li_2(L')_2(bpy)_2(H_2O)_6][Cu_2(HL)_2(bpy)_2(H_2O)_2](NO_3)_4$ (2): A colourless aqueous solution (2 mL) of LiOH·H$_2$O (0.018 g, 0.43 mmol) was added to a colourless solution of H$_2$L (0.050 g, 0.43 mmol) in MeCN (20 mL) to give a white suspension, which was stirred under heating for 50 min. Solid bpy (0.034 g, 0.22 mmol) was added, and the solution was stirred under heating for 1 h. A turquoise solution of $Cu(NO_3)_2·2.5H_2O$ (0.051 g, 0.22 mmol) in MeCN (10 mL) was then added to give a blue suspension, which was filtered off to obtain a final blue solution. X-ray quality, blue prismatic crystals of **1**·2H$_2$O were formed by layering of the blue solution with a mixture of Et$_2$O/*n*-hexane (10 mL, 1:1 v/v). The crystals were collected by filtration under vacuum, washed with cold MeCN (2 mL) and Et$_2$O (3 mL) and dried in air. Yield: 0.10 g (ca. 55%). FTIR for **1**·2H$_2$O (KBr pellet): $\tilde{\nu}$ = 3427 (w), 3334 (s br.), 3281 (w), 3201 (s br.), 3175 (m), 2341 (sh.), 1683 (s), 1650 (m), 1602 (vs), 1591 (vs), 1497 (w), 1474 (m), 1448 (s), 1424 (m), 1383 (vs), 1306 (s br.), 1250 (w), 1210 (w sh.), 1194 (w sh.), 1159 (w), 1106 (w), 1062 (w), 1034 (w), 1021 (w), 977 (vw), 927 (vw), 881 (vw), 828 (w br.), 771 (s), 729 (m), 668 (sh.), 652 (m), 625 (w), 499 (w), 475 (w) cm^{-1}. $C_{28}H_{32}Cu_2N_8O_{16}$ (863.70): calcd. C 38.94, H 3.74, N 12.97; found C 38.82, H 3.85, N 12.56.

Vapour diffusion of Et$_2$O onto the final blue solution of the reaction afforded blue prismatic crystals and needlelike dark blue crystals in an approximate ratio of 1:1, which were separated manually and dried in air. X-ray crystallography revealed that the blue prisms correspond to complex **1**·2H$_2$O (see above) and the dark blue needles correspond to complex **2**. FTIR for **2** (KBr pellet): $\tilde{\nu}$ = 3417 (s br.), 3176 (w), 2341 (w), 1680 (m), 1648 (w), 1603 (m), 1588 (s), 1498 (w), 1475 (m), 1448 (m), 1414 (m br.), 1383 (vs), 1312 (s), 1190 (w), 1064 (w), 1036 (m), 883 (w), 819 (m), 775 (m), 730 (m), 658 (m), 631 (w), 510 (w), 477 (w), 437 (w) cm^{-1}. $C_{56}H_{60}Cu_4Li_2N_{14}O_{34}$ (1741.22): calcd. C 38.63, H 3.47, N 11.26; found C 38.51, H 3.57, N 11.20.

Preparation of 1·2H$_2$O: A colourless aqueous solution (1.5 mL) of LiOH·H$_2$O (0.018 g, 0.43 mmol) was added to a colourless solution of H$_2$L (0.050 g, 0.43 mmol) in MeCN (20 mL) to give a white suspension. Solid bpy (0.034 g, 0.22 mmol) was added whilst heating. A turquoise solution of $Cu(NO_3)_2·2.5H_2O$ (0.051 g, 0.22 mmol) in MeCN (10 mL) was then added to give a blue suspension, which was filtered off to obtain a final blue solution. Slow evaporation of the solvent at room temperature afforded blue prismatic crystals after 7d, which were collected by filtration under vacuum, washed with cold MeCN (5 mL) and Et$_2$O (5 mL) and dried in air. Yield: 0.12 g (ca. 63%). The IR spectrum of this sample was identical with that reported above. $C_{28}H_{32}Cu_2N_8O_{16}$ (863.70): calcd. C 38.94, H 3.74, N 12.97; found C 38.92, H 3.65, N 12.76.

Preparation of $[Cu_2(HL)_2(bpy)_2(H_2O)_2](NO_3)_2$ (1) and $[Cu(L')(bpy)]_n·2nH_2O$ (4·2*n*H$_2$O): A colourless aqueous solution (1.5 mL) of LiOH·H$_2$O (0.018 g, 0.43 mmol) was added to a colourless solution of H$_2$L (0.050 g, 0.43 mmol) in MeCN (20 mL) to give a white suspension. Solid bpy (0.034 g, 0.22 mmol) was added to the above suspension, which was stirred whilst heating for 30 min. A turquoise solution of $Cu(NO_3)_2·2.5H_2O$ (0.051 g, 0.22 mmol) in MeCN (10 mL) was then added to the above suspension to obtain a final blue solution. Slow evaporation of the solvent at room temperature afforded blue prismatic crystals after 5 d, which were collected by filtration under vacuum, washed with Et$_2$O (4 mL) and dried in air. Yield: 0.11 g (ca. 60%). X-ray crystallography revealed that the blue prismatic crystals correspond to complex **1**. FTIR (KBr pellet): $\tilde{\nu}$ = 3427 (w), 3373 (w), 3281 (w), 3175 (m), 1682 (s), 1636 (sh.), 1591 (vs), 1497 (w), 1474 (m), 1449 (m), 1424 (m), 1370 (s br.), 1306 (s br.), 1250 (w), 1210 (w), 1194 (w), 1159 (w), 1106 (w), 1062 (w), 1034 (w), 1021 (w), 977 (vw), 927 (vw), 881 (vw), 828 (w br.), 771 (s), 729 (m), 668 (sh.), 652 (m), 625 (w), 499 (w), 475 (w) cm^{-1}. $C_{28}H_{28}Cu_2N_8O_{14}$ (827.66): calcd. C 40.63, H 3.41, N 13.54; found C 40.78, H 3.85, N 13.62.

Light blue needlelike crystals were formed upon standing of the final solution in a closed vial for 40 d. The crystals were collected by filtration under vacuum, washed with Et$_2$O (4 mL) and dried in air. Yield: 0.03 g (ca. 40%). X-ray crystallography revealed that the light blue crystals correspond to the known[7] complex **4**·2*n*H$_2$O.

Preparation of $[Cu_4(L')_2(NO_3)_2(bpy)_4(H_2O)_2](NO_3)_2·2H_2O$ (3·2H$_2$O)

Method A: A colourless aqueous solution (1.5 mL) of LiOH·H$_2$O (0.018 g, 0.43 mmol) was added to a colourless solution of H$_2$L (0.050 g, 0.43 mmol) in MeCN (20 mL) to give a white suspension. Solid bpy (0.034 g, 0.22 mmol) was added to the above suspension, which was stirred whilst heating for 30 min. A turquoise solution of $Cu(NO_3)_2·2.5H_2O$ (0.053 g, 0.22 mmol) in MeCN (10 mL) was then added to obtain a final blue solution. Blue prismatic crystals were formed after 10 d in a closed vial at ca. 4 °C. The crystals were collected by filtration under vacuum, washed with Et$_2$O (4 mL) and dried in air. Yield: 0.17 g (ca. 54%). X-ray crystallography revealed that the blue crystals correspond to complex **3**·2H$_2$O. FTIR for (KBr pellet): $\tilde{\nu}$ = 3450 (m), 1636 (w), 1590 (s), 1558 (s), 1496 (w), 1474 (w), 1442 (s), 1384 (s), 1316 (s), 1194 (w), 1160 (w), 1028 (w), 830 (m), 772 (m), 730 (w), 678 (w), 612 (w) cm^{-1}. $C_{48}H_{44}Cu_4N_{12}O_{24}$ (1427.13): calcd. C 40.40, H 3.11, N 11.78; found C 40.26, H 3.34, N 11.64.

Method B: Solid $[Cu_2(L')_2(bpy)_2]$·2MeOH (0.026 g, 0.036 mmol) was added to a light blue solution of $Cu(NO_3)_2·2.5H_2O$ (0.017 g, 0.072 mmol) in MeOH (11 mL) to give a darker blue suspension. Solid bpy (0.011 g, 0.072 mmol) was then added, and the resultant blue suspension was heated to reflux for 30 min to obtain a blue solution. X-ray quality blue prismatic crystals of **3**·2H$_2$O were formed by layering of the blue solution with Et$_2$O (10 mL). The crystals were collected by filtration under vacuum, washed with cold MeOH (2 mL) and Et$_2$O (3 mL) and dried in air. Yield: 0.11 g (ca. 55%). The IR spectrum of this sample was identical to the spectrum of the sample prepared by method A. $C_{48}H_{44}Cu_4N_{12}O_{24}$ (1427.13): calcd. C 40.40, H 3.11, N 11.78; found C 40.16, H 3.29, N 11.49.

Preparation of $[Cu_4(L')_2(NO_3)_2(bpy)_4(H_2O)_2](NO_3)_2·2[Li(NO_3)(H_2O)_3]·4H_2O$ (5·4H$_2$O), $[Cu(NO_3)(bpy)(H_2O)_3](NO_3)$ (6) and 4·2*n*H$_2$O: A colourless aqueous solution (3 mL) of LiOH·H$_2$O (0.037 g, 0.88 mmol) was added to a colourless solution of H$_2$L′ (0.051 g, 0.44 mmol) in MeCN (25 mL) to give a white suspension. Solid bpy (0.069 g, 0.44 mmol) was added to the above suspension. A greenish-turquoise solution of $Cu(NO_3)_2·2.5H_2O$ (0.102 g, 0.44 mmol) in MeCN (15 mL) was then added to give a light blue suspension, which was filtered off; the final light blue solution was layered with a mixture of Et$_2$O/*n*-hexane (10 mL, 1:1 v/v). X-ray quality light blue-greenish and blue prismatic crystals in an approximate ratio of 1:1 were formed, which were separated manually and dried in air. X-ray crystallography revealed that the blue prisms correspond to complex **5**·4H$_2$O and the light blue-greenish plates correspond to the known[9] complex **6**. FTIR for **5**·4H$_2$O (KBr pellet): $\tilde{\nu}$ = 3421 (s br.), 3108 (w), 1733 (w), 1647 (w), 1589 (vs), 1558 (vs), 1495 (m), 1473 (m), 1446 (s), 1384 (vs), 1352 (sh.), 1315 (sh.), 1250 (w), 1198 (w), 1175 (w), 1158 (m), 1057 (m), 1032 (m), 1017 (sh.), 913 (w), 860 (vw), 843 (m), 773 (s), 730 (s), 650 (w), 609 (w br.), 417 (m) cm^{-1}. $C_{48}H_{60}Cu_4Li_2N_{14}O_{38}$ (1709.14): calcd. C 33.73, H 3.54, N 11.47; found C 33.63, H 3.57, N 11.42.

Table 1. Crystallographic data for complexes **1**, **1**·2H_2O, **2**, **3**·2H_2O and **5**·4H_2O.

	1	**1**·2H_2O	**2**	**3**·2H_2O	**5**·4H_2O
*F*ormula	$C_{28}H_{28}Cu_2N_8O_{14}$	$C_{28}H_{32}Cu_2N_8O_{16}$	$C_{56}H_{60}Cu_4Li_2N_{14}O_{34}$	$C_{48}H_{44}Cu_4N_{12}O_{24}$	$C_{48}H_{60}Cu_4Li_2N_{14}O_{38}$
F_w	827.66	863.70	1741.22	1427.13	1709.14
Space group	$P2_1/c$	$P\bar{1}$	$P\bar{1}$	$Pn2_1a$	$C2/c$
a [Å]	8.995(5)	9.368(5)	9.07(1)	16.409(4)	31.53(1)
b [Å]	19.89(1)	10.251(5)	19.39(2)	13.261(3)	10.312(4)
c [Å]	9.359(6)	11.283(6)	9.88(1)	26.218(6)	24.390(9)
α [°]	90.00	63.99(2)	92.27(4)	90.00	90.00
β [°]	95.76(2)	75.83(2)	90.86(4)	90.00	120.94(2)
γ [°]	90.00	63.64(2)	93.34(3)	90.00	90.00
V [Å^3]	1666.5(17)	870.8(8)	1734(3)	5705(2)	6802(4)
Z	2	1	1	4	4
T [°C]	20	25	25	25	25
Radiation	Cu-K_α	Mo-K_α	Cu-K_α	Mo-K_α	Mo-K_α
$\rho_{calcd.}$ [g cm^{-3}]	1.649	1.647	1.667	1.662	1.669
μ [mm^{-1}]	2.294	1.307	2.290	1.565	1.342
R_1[a]	0.0359[b]	0.0412[c]	0.0461[d]	0.0339[e]	0.0467[f]
wR_2[a]	0.0971[b]	0.1018[c]	0.1211[d]	0.0894[e]	0.1173[f]

[a] $w = 1/[\sigma^2(F_o^2)+(aP)^2+bP]$ and $P = [\max(F_o^2,0) + 2F_c^2]/3$, $R_1 = \Sigma(|F_o| - |F_c|)/\Sigma(|F_o|)$ and $wR_2 = \{\Sigma[w(F_o^2 - F_c^2)^2]/\Sigma[w(F_o^2)^2]\}^{1/2}$. [b] For 2239 reflections with $I > 2\sigma(I)$. [c] For 2786 reflections with $I > 2\sigma(I)$. [d] For 4167 reflections with $I > 2\sigma(I)$. [e] For 7528 reflections with $I > 2\sigma(I)$. [f] For 4565 reflections with $I > 2\sigma(I)$.

Light blue needlelike crystals were formed upon standing of the final light blue solution in a closed vial at ca. 4 °C. The crystals were collected by filtration under vacuum, washed with cold MeCN (3 mL) and Et_2O (4 mL) and dried in air. X-ray crystallography revealed that the light blue needles correspond to the known complex[7] **4**·2*n*H_2O.

X-ray Crystallography: Blue prismatic crystals of **1** (0.20 × 0.25 × 0.35 mm), **1**·2H_2O (0.10 × 0.25 × 0.50 mm), **2** (0.06 × 0.15 × 0.25 mm), **3**·2H_2O (0.30 × 0.35 × 0.50 mm) and **5**·4H_2O (0.20 × 0.30 × 0.60 mm) were mounted in capillaries. Diffraction measurements were made on a Crystal Logic Dual Goniometer diffractometer (for **1**·2H_2O, **3**·2H_2O and **5**·4H_2O) by using graphite monochromated Mo-K_α radiation and on a $P2_1$ Nicolet diffractometer upgraded by Crystal Logic (for **1** and **2**) by using graphite monochromated Cu-K_α radiation. Unit cell dimensions were determined by using the angular settings of 25 automatically centred reflections in the range $11 < 2\theta < 23°$ (for **1**·2H_2O, **3**·2H_2O and **5**·4H_2O) and $22 < 2\theta < 54°$ (for **1** and **2**). Intensity data were recorded using a θ–2θ scan. Three standard reflections monitored every 97 reflections showed less than 3% variation and no decay. Lorentz, polarization and psi-scan absorption corrections (for **5**·4H_2O) were applied by using Crystal Logic software. Important crystallographic and refinement data are listed in Table 1. The structures were solved by direct methods with SHELXS-97[22] and refined by full-matrix least-squares techniques on F^2 with SHELXL-97.[23] Further crystallographic details for **1**: $2\theta_{max}$ = 118°; reflections collected/unique/used 2562/2397 [R_{int} = 0.0164]/2397; 292 parameters refined; $(\Delta/\sigma)_{max}$ = 0.001; $(\Delta\rho)_{max}/(\Delta\rho)_{min}$ = 0.533/–0.383 e/Å^3; R/R_w (for all data) 0.0376/0.0989. Hydrogen atoms were located by difference maps and were refined isotropically. All non-H atoms were refined anisotropically. Further crystallographic details for **1**·2H_2O: $2\theta_{max}$ = 50°; reflections collected/unique/used 3266/3062 [R_{int} = 0.0261]/3062; 308 parameters refined; $(\Delta/\sigma)_{max}$ = 0.001; $(\Delta\rho)_{max}/(\Delta\rho)_{min}$ = 0.519/–0.454 e/Å^3; R/R_w (for all data) 0.0466/0.1061. Hydrogen atoms were located by difference maps and were refined isotropically. All non-H atoms were refined anisotropically. Further crystallographic details for **2**: $2\theta_{max}$ = 118°; reflections collected/unique/used 5133/4800 [R_{int} = 0.0197]/4800; 578 parameters refined; $(\Delta/\sigma)_{max}$ = 0.003; $(\Delta\rho)_{max}/(\Delta\rho)_{min}$ = 0.370/–0.698 e/Å^3; R/R_w (for all data) 0.0530/0.1288. Hydrogen atoms were either located by difference maps and refined isotropically or introduced at calculated positions as riding on bonded atoms. All non-H atoms were refined anisotropically. Further crystallographic details for **3**·2H_2O: $2\theta_{max}$ = 50°; reflections collected/unique/used 8306/8306 [R_{int} = 0.0000]/8306; 826 parameters refined; $(\Delta/\sigma)_{max}$ = 0.004; $(\Delta\rho)_{max}/(\Delta\rho)_{min}$ = 0.876/–0.265 e/Å^3; R/R_w (for all data) 0.0405/0.0939. Hydrogen atoms were either located by difference maps and refined isotropically or introduced at calculated positions as riding on bonded atoms. All non-H atoms were refined anisotropically. Further crystallographic details for **5**·4H_2O: $2\theta_{max}$ = 48°; reflections collected/unique/used 5461/5313 [R_{int} = 0.0414]/5313; 551 parameters refined; $(\Delta/\sigma)_{max}$ = 0.005; $(\Delta\rho)_{max}/(\Delta\rho)_{min}$ = 1.905/–0.721 e/Å^3; R/R_w (for all data) 0.0571/0.1259. Hydrogen atoms were either located by difference maps and refined isotropically or introduced at calculated positions as riding on bonded atoms. All non-H atoms were refined anisotropically. Plots of all structures were drawn by using the Diamond 3 program package.[24] CCDC-734072 (**1**·2H_2O), -734073 (**1**), -734074 (**2**), -734075 (**3**·2H_2O) and -734076 (**5**·4H_2O) contain the supplementary crystallographic data for this paper. These data can be obtained free of charge from The Cambridge Crystallographic Data Centre via www.ccdc.cam.ac.uk/data_request/cif.

Supporting Information (see footnote on the first page of this article): Molecular structure of the cation of **1**·2H_2O; selected interatomic bond lengths [Å] and angles [°], hydrogen-bonding interactions and diagnostic amide and carboxylate IR bands for complexes **1**, **1**·2H_2O, **2**, **3**·2H_2O and **5**·4H_2O.

Acknowledgments

S. P. P. thanks the Research Committee of the University of Patras for support (K. Caratheodory Program No 03016).

[1] For reviews see: a) A. J. Tasiopoulos, S. P. Perlepes, *Dalton Trans.* **2008**, 5537–5555; b) G. Christou, *Polyhedron* **2005**, *24*,1809; c) E. K. Brechin, *Chem. Commun.* **2005**, 5141–5153; d) R. E. P. Winpenny in *Comprehensive Coordination Chemistry II* (Eds.: J. A. McCleverty, T. J. Meyer), vol. 7, Elsevier, Amsterdam, **2004**, pp. 125–175.

[2] For reviews see: a) D.-K. Bučar, G. S. Papaefstathiou, T. D. Hamilton, Q. L. Chu, I. G. Georgiev, L. R. McGillivray, *Eur. J. Inorg. Chem.* **2007**, 4559–4568; b) A. Y. Robin, K. M. Fromm, *Coord. Chem. Rev.* **2006**, *250*, 2127–2157; c) S. Kitaqawa, S. Noro in *Comprehensive Coordination Chemistry II* (Eds.: J. A. McClevert, T. J. Meyer), vol. 7, Elsevier, Amsterdam, **2004**, pp. 231–261; d) C. Janiak, *Dalton Trans.* **2003**, 2781–2804.
[3] See for example: C. N. R. Rao, S. Natarajan, R. Vaidhyanathan, *Angew. Chem. Int. Ed.* **2004**, *43*, 1466–1496 and references cited therein.
[4] For example see: a) D. Ghoshal, T. K. Maji, G. Mostafa, S. Sain, T.-H. Lu, J. Ribas, E. Zangrando, N. R. Chaudhuri, *Dalton Trans.* **2004**, 1687–1695; b) Y. Y. Wang, X. Wang, Q. Z. Shi, Y. C. Gao, *Transition Met. Chem.* **2002**, *27*, 481–484; c) M. Geraghty, M. McCann, M. T. Casey, M. Curran, M. Devereux, V. McKee, J. McCrea, *Inorg. Chim. Acta* **1998**, *277*, 257–262; d) M. McCann, M. T. Casey, M. Devereux, M. Curran, V. McKee, *Polyhedron* **1997**, *16*, 2741–2748.
[5] I. Chadjistamatis, A. Terzis, C. P. Raptopoulou, S. P. Perlepes, *Inorg. Chem. Commun.* **2003**, *6*, 1365–1371.
[6] a) K. N. Lazarou, I. Chadjistamatis, V. Psycharis, S. P. Perlepes, C. P. Raptopoulou, *Inorg. Chem. Commun.* **2007**, *10*, 318–323; b) K. N. Lazarou, S. P. Perlepes, V. Psycharis, C. P. Raptopoulou, *Polyhedron* **2008**, *27*, 2131–2142; c) K. N. Lazarou, V. Psycharis, S. P. Perlepes, C. P. Raptopoulou, *Polyhedron* **2009**, *28*, 1085–1096.
[7] a) C. Zhang, J. Sun, X. Kong, C. Zhao, *J. Coord. Chem.* **2000**, *49*, 181–188; b) K.-L. Zhang, Y. Xu, J.-G. Lin, X.-Z. You, *J. Mol. Struct.* **2004**, *703*, 63–67.
[8] E. C. Constable, *Metals and Ligand Reactivity*, VCH, Weinheim, **1996**, pp. 46–56, pp. 65–72.
[9] L. Jianmin, Z. Jianbin, K. Yanxiong, W. Xintao, *Cryst. Res. Technol.* **1996**, *31*, 589–593.
[10] M. Albrecht, I. Janser, J. Runsink, G. Raabe, P. Weis, R. Fröchlich, *Angew. Chem. Int. Ed.* **2004**, *43*, 6662–6666.
[11] C. Gkioni, A. K. Boudalis, Y. Sanakis, L. Leondiadis, V. Psycharis, C. P. Raptopoulou, *Polyhedron* **2008**, *27*, 2315–2326.
[12] G. Christou, S. P. Perlepes, E. Libby, K. Folting, J. C. Huffman, R. J. Webb, D. N. Hendrickson, *Inorg. Chem.* **1990**, *29*, 3657–3666.
[13] J.-P. Costes, F. Dahan, J.-P. Laurent, *Inorg. Chem.* **1985**, *24*, 1018–1022.
[14] A. W. Addison, T. N. Rao, J. Reedijk, J. Rijn, G. C. Verschoor, *J. Chem. Soc., Dalton Trans.* **1984**, 1349–1356.
[15] C. Papatriantafyllopoulou, C. P. Raptopoulou, A. Terzis, J. F. Janssens, E. Manesssi-Zoupa, S. P. Perlepes, J. C. Plakatouras, *Polyhedron* **2007**, *26*, 4053–4064.
[16] A. K. Boudalis, V. Nastopoulos, S. P. Perlepes, C. P. Raptopoulou, A. Terzis, *Transition Met. Chem.* **2001**, *26*, 276–281.
[17] K. Nakamoto, *Infrared and Raman Spectra of Inorganic and Coordination Compounds*, 4th ed., Wiley, New York, **1986**.
[18] G. B. Deacon, R. J. Phillips, *Coord. Chem. Rev.* **1980**, *33*, 227–250.
[19] a) J. Aussoleil, P. Cassoux, P. de Loth, J.-P. Tuchagues, *Inorg. Chem.* **1989**, *28*, 3051–3056; b) J. M. Clemente-Juan, C. Mackiewicz, M. Verelst, F. Dahan, A. Bousseksou, Y. Sanakis, J.-P. Tuchagues, *Inorg. Chem.* **2002**, *41*, 1478–1491.
[20] *MINUIT Program, A System for Function Minimization and Analysis of the Parameters Errors and Correlations* F. James, M. Roos, *Comput. Phys. Commun.* **1975**, *10*, 343–367.
[21] a) J. J. Borrás-Almenar, J. M. Clemente-Juan, E. Coronado, B. S. Tsukerblat, *Inorg. Chem.* **1999**, *38*, 6081–6088; b) J. J. Borrás-Almenar, J. M. Clemente-Juan, E. Coronado, B. S. Tsukerblat, *J. Comput. Chem.* **2001**, *22*, 985–991.
[22] G. M. Sheldrick, *SHELXS-97, Structure Solving Program*, University of Göttingen, Germany, **1997**.
[23] G. M. Sheldrick, *SHELXL-97, Crystal Structure Refinement Program*, University of Göttingen, Germany, **1997**.
[24] *DIAMOND – Crystal and Molecular Structure Visualization*, Version 3.1, Crystal Impact, Rathausgasse 30, 53111, Bonn, Germany.

Received: May 29, 2009
Published Online: September 1, 2009

